Biophysical Journal, Volume *117*

Supplemental Information

Atomistic Insights into the Functional Instability of the Second Helix of Fatty Acid Binding Protein

Peng Cheng, Dan Liu, Pin Xuan Chee, Daiwen Yang, and Dong Long

Supporting Material

SUPPORTING METHODS

System preparation for aMD

The simulation was conducted using the AMBER 14 software package (1), employing the AMBER ff99SBnmr1-ILDN force field (2, 3). The crystal structure of human IFABP (PDB code: 3AKM) was used as the starting conformation, and the bound ligand and Mg^{2+} in the crystal structure were removed. The system was solvated in a truncated octahedral box with 10 Å distance between our system and the box edges, with the TIP3P water model (4). As the protein is electrically neutral, no ions were added. The system temperature was maintained at 300 K using the Langevin thermostat with a collision frequency of 2.0 ps^{-1}. The time step of the simulation was 2 fs. The pressure was coupled to 1 bar using isotropic position scaling with a relaxation time of 1.0 ps. The SHAKE algorithm (5) was applied to constrain all the bonds involving hydrogen atoms. PME (6) was used for the long-range electrostatic interactions with a 10 Å cutoff for the long range non-bonded interactions. The system was relaxed by the energy minimization and equilibration procedures as described previously (7). The production run of aMD and a short (100 ns) convention MD simulations were carried out under the NPT condition. The average total and dihedral potential energies were calculated from the 100 ns MD trajectory for determining the boost parameters ($\langle V_{total} \rangle = -50968$ kcal·mol^{-1}, $\langle V_{dihed} \rangle = 1606$ kcal·mol^{-1}).

SUPPORTING FIGURES

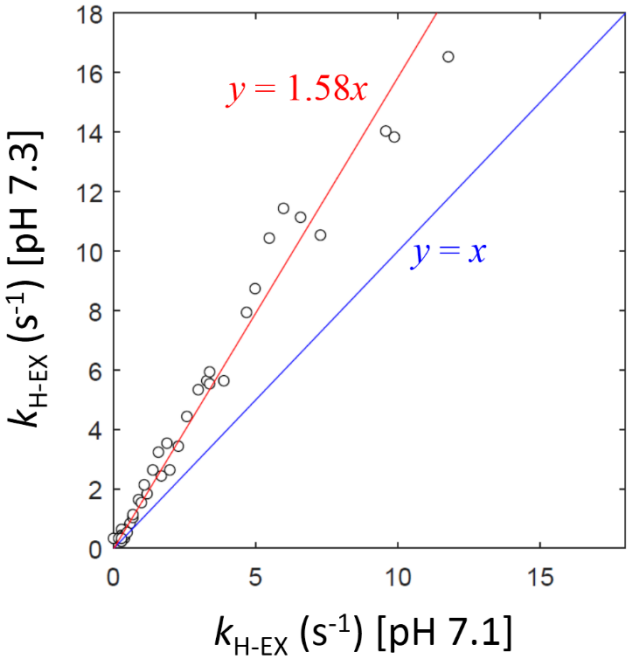

FIGURE S1. Comparison of the amide hydrogen exchange rates measured at pH 7.3 and 7.1. The Pearson correlation coefficient of the two data sets is 0.987. The increase of $k_{H\text{-}EX}$ from pH 7.1 to 7.3 agrees with the theoretical prediction of the EX2 model (1.58-fold). Data at pH 7.1 were taken from the previous work (8).

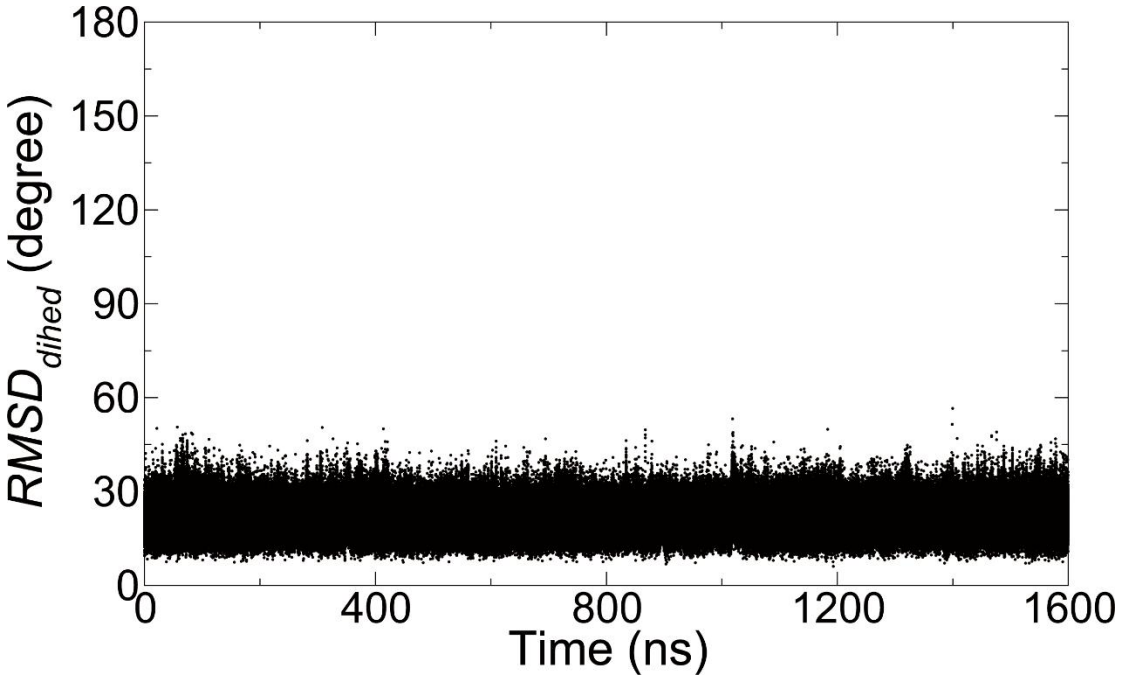

FIGURE S2. $RMSD_{dihed}$ of αII (residues 24-32) with respect to the initial conformation, calculated from the 1.6 μs MD trajectory of human IFABP simulated at 300 K.

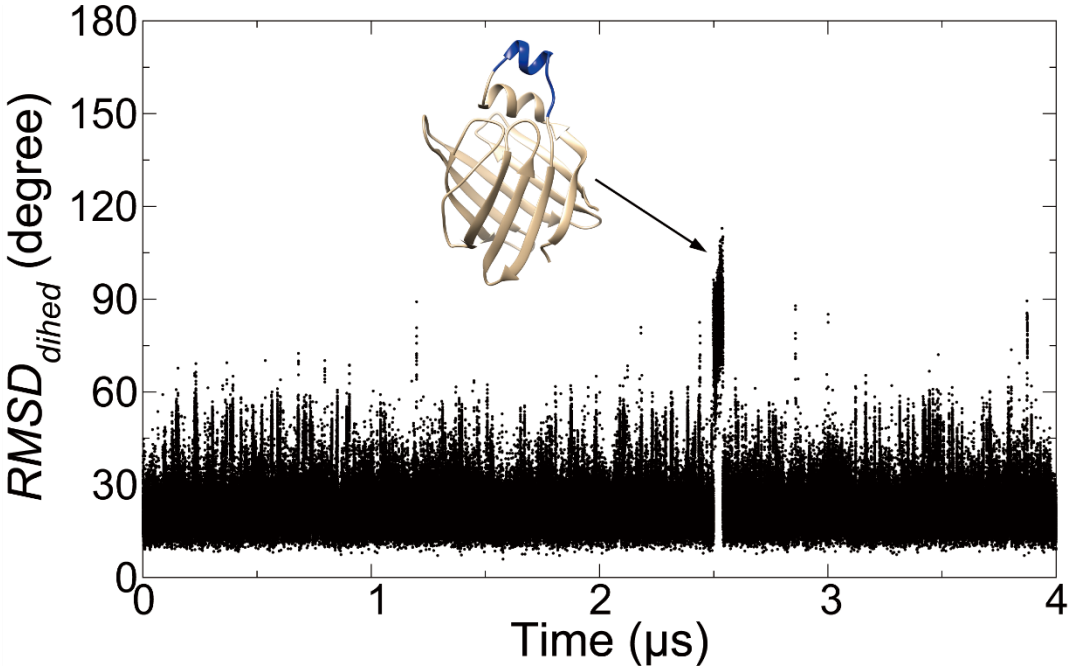

FIGURE S3. $RMSD_{dihed}$ of the second helix of rat IFABP (residues 24-33) with respect to the initial conformation in a 4 μs MD simulation at 350 K. The crystal structure of rat IFABP (PDB code: 1IFB) was used as the starting structure for the simulation, and the system setup was fully analogous to that of human IFABP.

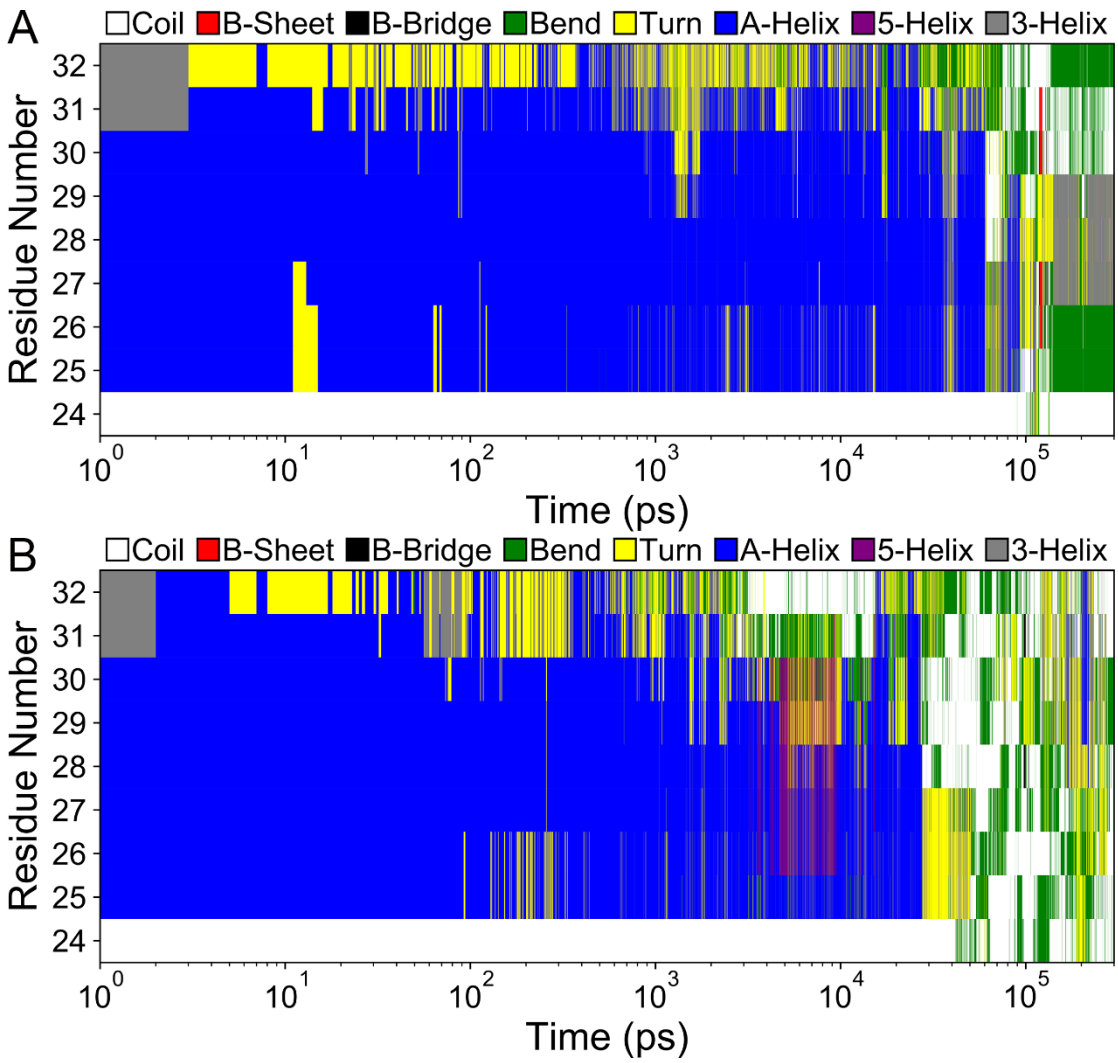

FIGURE S4. Variation of secondary structures of individual residues of αII (human IFABP) in two independent well-tempered metadynamics simulations with bias factors set to 3 (A) and 15 (B). The x-axes are shown on a logarithmic scale.

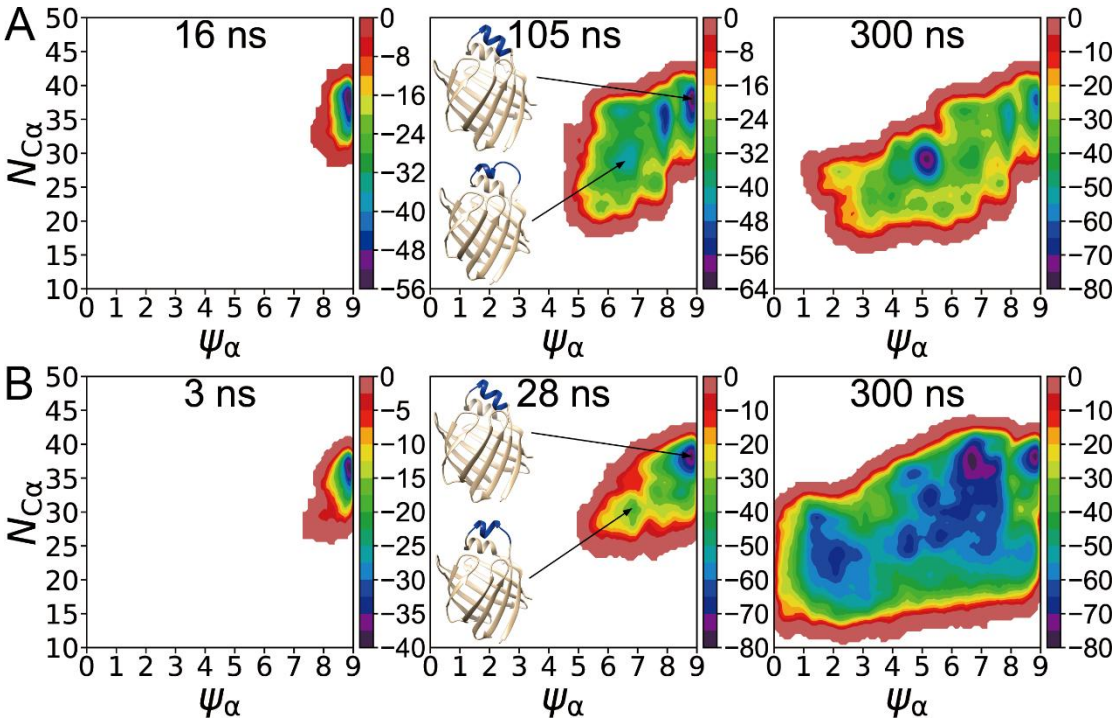

FIGURE S5. Estimates of free energy surfaces (kJ/mol) at different simulation times in well-tempered metadynamics with the bias factors set to 3 (A) and 15 (B).

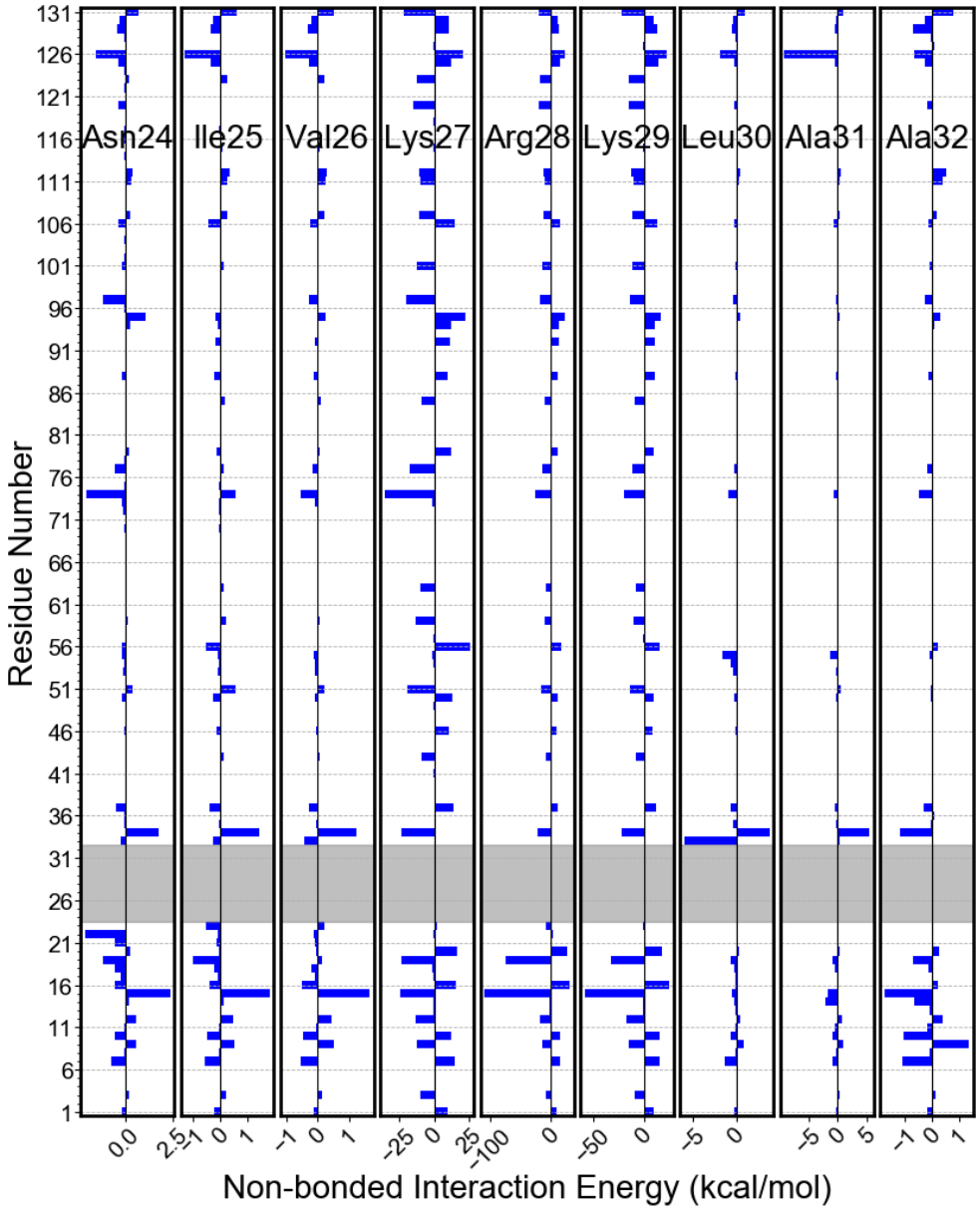

FIGURE S6. The non-bonded interaction energies (kcal/mol) between all pairs of residues belonging to αII and the rest of the protein respectively in the native conformation. The shaded area (grey) indicates the αII region (residues 24-32). Each panel shows the interactions between a specific residue of αII and those from the non-αII regions. Interaction energies between neighboring residues are not shown.

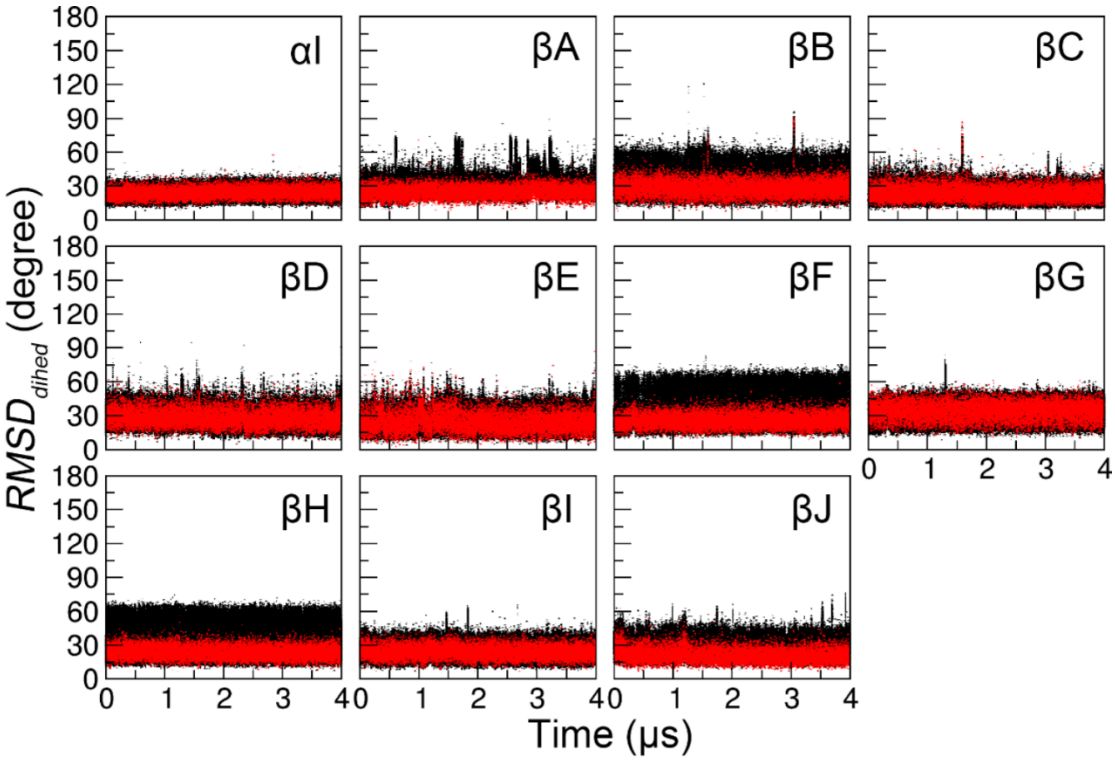

FIGURE S7. $RMSD_{dihed}$ of individual secondary structural elements (other than αII) of human IFABP during the MD simulation at 350 K. The first and last residues of individual secondary structural elements were included (black) or excluded (red) for the calculations. The non-terminal regions of these secondary structural elements were found to be stable throughout the simulation, although fraying of the first or last residue was common. Transient fraying of the second or the second last residues was also observed in βC and βB, respectively.

Table S1. Summary of individual simulations performed in this work.

Systems	Method	Temperature (K)	Simulation time (μs)
capped αI	MD	300	10
capped αII	MD	300	10
human IFABP	MD	300	1.6
	MD	350	4
rat IFABP	MD	350	4
human IFABP	Well-tempered metadynamics (γ=6)	300	1.15
	Well-tempered metadynamics (γ=3)	300	0.3
	Well-tempered metadynamics (γ=15)	300	0.3
human IFABP	aMD	300	5

Table S2. Amide hydrogen exchange rates[a] of human IFABP.

Residue	$k_{H\text{-}EX}$ (s^{-1})[b]	Errors of $k_{H\text{-}EX}$ (s^{-1})	k_{rc} (s^{-1})[c]	Protection factor ($k_{rc}/k_{H\text{-}EX}$)	Population of the open form ($k_{H\text{-}EX}/k_{rc}$)	Location in secondary structures
2	0.8	0.1	687	9.E+02	1.E-03	
3	0.6	0.1	30.1	5.E+01	2.E-02	
4	0.6	0.1	80.8	1.E+02	7.E-03	βA
5	1.8	0.1	88.4	4.9E+01	2.0E-02	
11	5.6	0.2	202	3.6E+01	2.8E-02	
12	0.3	0.1	32.2	1.E+02	9.E-03	
14	2.4	0.1	58.4	2.4E+01	4.1E-02	αI
16	1.0	0.1	31.5	3.2E+01	3.2E-02	
23	0.3	0.1	15.4	5.E+01	2.E-02	
24	11.4	0.3	117	1.03E+01	9.74E-02	αII
25	7.9	0.2	20.3	2.6E+00	3.9E-01	
26	1.1	0.1	6.1	5.6E+00	1.8E-01	
27	3.4	0.1	34.4	1.0E+01	9.9E-02	
28	5.5	0.2	82.5	1.5E+01	6.7E-02	
29	11.1	0.4	78.8	7.10E+00	1.41E-01	
30	2.6	0.1	18	6.9E+00	1.4E-01	
31	3.5	0.1	32.1	9.2E+00	1.1E-01	
32	5.9	0.2	52.1	8.8E+00	1.1E-01	
33	8.7	0.2	65.2	7.5E+00	1.3E-01	
34	5.3	0.2	51.3	9.7E+00	1.0E-01	
35	5.6	0.1	107	1.9E+01	5.2E-02	
36	0.4	0.1	28.6	7.E+01	1.E-02	
42	0.4	0.1	94.7	2.E+02	4.E-03	βB
43	0.3	0.1	25.6	9.E+01	1.E-02	
45	13.8	0.4	238	1.72E+01	5.80E-02	
54	10.4	0.4	104	1.00E+01	1.00E-01	
55	3.2	0.1	30	9.4E+00	1.1E-01	
56	1.6	0.1	71.8	4.5E+01	2.2E-02	
58	0.2	0.1	20.3	1.E+02	1.E-02	βD
59	2.1	0.1	9.5	4.5E+00	2.2E-01	
67	10.5	0.3	32.1	3.06E+00	3.27E-01	
71	1.5	0.1	180	1.2E+02	8.3E-03	βE
75	4.4	0.2	64.2	1.5E+01	6.9E-02	
76	2.6	0.2	65.5	2.5E+01	4.0E-02	
77	0.2	0.1	25.6	1.E+02	8.E-03	βF
87	14	0.4	238	1.7E+01	5.9E-02	
96	2.1	0.1	73.5	3.5E+01	2.9E-02	
97	0.4	0.1	41.5	1.E+02	1.E-02	

98	0.5	0.1	107	2.E+02	5. E-03	
99	0.3	0.1	202	7.E+02	2.E-03	
110	16.5	0.4	57.1	3.46E+00	2.89E-01	
120	0.4	0.1	18.1	5.E+01	2.E-02	
121	0.2	0.1	68.8	3.E+02	3.E-03	

[a] Only the residues with amide hydrogen exchange rates $\geq 0.2\ s^{-1}$ are listed in the table. The hydrogen exchange rates smaller than $0.2\ s^{-1}$ could not be reliably measured using the selective water inversion scheme. The protection factors of the residues with $k_{H\text{-}EX} < 0.2\ s^{-1}$ are significantly larger than 200.

[b] To calculate $k_{H\text{-}EX}$, the proton longitudinal relaxation rate of water and the fraction of recovered water magnetization were measured, which were $0.3\ s^{-1}$ and 0.8, respectively.

[c] The hydrogen exchange rates for random coils (k_{rc}) were predicted using SPHERE (http://landing.foxchase.org/research/labs/roder/sphere/sphere.html).

References

1. Case, D.A., V. Babin, J.T. Berryman, R.M. Betz, Q. Cai, D.S. Cerutti, T.E. Cheatham, T.A. Darden, R.E. Duke, H. Gohlke, A.W. Goetz, S. Gusarov, N. Homeyer, P. Janowski, J. Kaus, I. Kolossváry, A. Kovalenko, T.S. Lee, S. LeGrand, T. Luchko, R. Luo, B. Madej, K.M. Merz, F. Paesani, D.R. Roe, A. Roitberg, C. Sagui, R. Salomon-Ferrer, G. Seabra, C.L. Simmerling, W. Smith, J. Swails, Walker, J. Wang, R.M. Wolf, X. Wu, and P.A. Kollman. 2014. Amber 14, University of California, San Francisco. .
2. Lindorff-Larsen, K., S. Piana, K. Palmo, P. Maragakis, J.L. Klepeis, R.O. Dror, and D.E. Shaw. 2010. Improved side-chain torsion potentials for the Amber ff99SB protein force field. *Proteins: Struct. Funct. Bioinform.* 78: 1950–1958.
3. Long, D., D.W. Li, K.F.A. Walter, C. Griesinger, and R. Brüschweiler. 2011. Toward a predictive understanding of slow methyl group dynamics in proteins. *Biophys. J.* 101: 910–915.
4. Jorgensen, W.L., J. Chandrasekhar, J.D. Madura, R.W. Impey, and M.L. Klein. 1983. Comparison of simple potential functions for simulating liquid water. *J. Chem. Phys.* 79: 926–935.
5. Ryckaert, J.-P., G. Ciccotti, and H.J.. Berendsen. 1977. Numerical integration of the cartesian equations of motion of a system with constraints: molecular dynamics of n-alkanes. *J. Comput. Phys.* 23: 327–341.
6. Essmann, U., L. Perera, M.L. Berkowitz, T. Darden, H. Lee, and L.G. Pedersen. 1995. A smooth particle mesh Ewald method. *J. Chem. Phys.* 103: 8577–8593.
7. Cheng, P., J. Peng, and Z. Zhang. 2017. SAXS-Oriented Ensemble Refinement of Flexible Biomolecules. *Biophys. J.* 112: 1295–1301.
8. Yu, B., and D. Yang. 2016. Coexistence of multiple minor states of fatty acid binding protein and their functional relevance. *Sci. Rep.* 6: 34171.